Hyperpolarized Magnetic Resonance Shows that the Anti-Ischemic Drug, Meldonium, Leads to Increased Flux Through Pyruvate Dehydrogenase In Vivo Resulting in Improved Post-Ischemic Function in the Diabetic Heart.

Dragana Savic (dragana.savic@cardiov.ox.ac.uk)
University of Oxford https://orcid.org/0000-0003-1038-4100
Vicky Ball
University of Oxford
Lorenz Holzner
University of Cambridge
David Hauton
University of Oxford
Kerstin Timm
University of Oxford
M. Kate Curtis
University of Oxford
Lisa C. Heather
University of Oxford
Damian J. Tyler
University of Oxford

Original investigation

Keywords: Meldonium, Mildronate, L-Carnitine, Streptozotocin, Cardiovascular Disease, Ischemia-Reperfusion, Heart, Type-1 Diabetes, Hyperpolarized Magnetic Resonance

Posted Date: August 5th, 2020

DOI: https://doi.org/10.21203/rs.3.rs-47558/v1

Version of Record: A version of this preprint was published at NMR in Biomedicine on January 17th, 2021. See the published version at https://doi.org/10.1002/nbm.4471.

Abstract

Background: The diabetic heart has a decreased ability to metabolize glucose. The anti-ischemic drug, Meldonium, may provide a route to counteract this by reducing L-carnitine levels, resulting in improved cardiac glucose utilization. Therefore, the aim of this study was to use the novel technique of hyperpolarized magnetic resonance to investigate the *in vivo* effects of treatment with Meldonium on cardiac metabolism and function in control and diabetic rats.

Methods: 36 male Wistar rats were injected with either placebo or streptozotocin (55mg/kg) to induce a model of type-1 diabetes. Daily treatment with either saline or Meldonium (100mg/kg/day) was undertaken for three weeks. *In vivo* cardiac function and metabolism were assessed with CINE MRI and hyperpolarized magnetic resonance respectively. Isolated perfused hearts were challenged with low-flow ischemia/reperfusion to assess the impact of Meldonium on post-ischemic recovery.

Results: Meldonium had no significant effect on blood glucose levels or on baseline cardiac function. However, hyperpolarized magnetic resonance revealed that Meldonium treatment elevated pyruvate dehydrogenase flux by 3.1-fold and 1.2-fold in diabetic and control animals respectively, indicating an increase in cardiac glucose oxidation. Hyperpolarized magnetic resonance further demonstrated that Meldonium reduced acetylcarnitine by 2.1-fold in both diabetic and control animals. The increase in *in vivo* glucose oxidation was accompanied by an improvement in *ex vivo* post-ischemic function, where Meldonium elevated rate pressure product by 1.3-fold and 1.5-fold in the control and diabetic animals respectively.

Conclusion: Meldonium improves *in vivo* glucose utilization in the diabetic heart, contributing to improved cardiac recovery post-ischemia.

Background

Diabetes has become increasingly prevalent in recent years with a global incidence estimated to rise from 108 million people in 1980 to 700 million people in 2045[1]. Of these people, it is suggested that 5-15% will have type-1 diabetes (T1D)[2]. Diabetes is associated with an elevated risk of cardiovascular disease and heart failure[3,4], and cardiovascular disease is the major cause of premature death in diabetic patients[5]. Therefore, therapies that protect the heart in diabetes are urgently needed to reduce this mortality.

Dysregulated cardiac substrate utilization and mitochondrial dysfunction are contributing factors to impaired cardiac function in the diabetic population[6,7]. In the healthy heart, 60–70% of ATP production comes from fatty acids (FAs), and the remaining 30–40% comes from glucose and lactate. However, in diseases such as diabetes, this balance is shifted even further in favour of fatty acid oxidation[8,9]. Therefore, drugs that target this metabolic imbalance in the diabetic heart are of great therapeutic interest. One such drug is the anti-ischemic agent Meldonium (trimethylhydrazinium propionate), which is sold under the brand name Mildronate. The anti-ischemic actions of Meldonium are thought to originate from a switch in the balance of fuel utilization in the heart towards more oxygen-efficient glucose metabolism. These effects arise from the impact of Meldonium on the synthesis and transport of the amino acid derivative, L-carnitine.

L-carnitine is required for the transport of long-chain FAs into mitochondria via the carnitine shuttle. L-carnitine accepts the fatty acid moiety from long-chain acyl-CoAs found in the cytoplasm, making them a suitable substrate for mitochondrial uptake via the carnitine-acylcarnitine translocase within the inner mitochondrial membrane. Meldonium has been shown to reduce L-carnitine availability both through inhibition of the L-carnitine transporter, OCTN2, inhibiting absorption and reabsorption of L-carnitine in tissues, as well as through inhibition of the last step in the biosynthesis of L-carnitine; Y-butyrobetaine hydroxylase.

As such, treatment with Meldonium can be hypothesized to reduce fatty acid uptake and oxidation in the mitochondrial matrix and provide a drive to increase glucose oxidation via the Randle cycle[10,11], primarily through reduced acetyl-CoA availability, which is known to inhibit glucose oxidation at the key regulatory step of Pyruvate Dehydrogenase (PDH)[12]. In a proof-of-concept study, we have shown previously that therapeutic strategies that improve mitochondrial pyruvate oxidation via increased PDH activity result in improved cardiac function in diabetes[13]. However, clinically relevant compounds that improve cardiac PDH flux in diabetes are lacking. By modulating carnitine availability, Meldonium may therefore provide a route to improve cardiac glucose utilization via increased PDH flux in diabetes.

This study aimed to investigate the effects of Meldonium on *in vivo* cardiac metabolism and function in control and diabetic rodent hearts, using hyperpolarized magnetic resonance spectroscopy (MRS) and CINE magnetic resonance imaging (MRI), respectively. Hyperpolarized MRS is a novel technique, which can increase the *in vivo* sensitivity of MRS to detect ^{13}C-labelled metabolic substrates by more than 10,000-fold[14]. It therefore enables unprecedented real-time visualization of the biochemical mechanisms of normal and abnormal metabolism, with measurement of instantaneous substrate uptake and enzymatic transformation *in vivo*[15]. Following the injection of ^{13}C pyruvate labelled at the first carbon position ([1-^{13}C]pyruvate), it is possible to see the metabolic production of carbon dioxide and bicarbonate ($^{13}CO_2$ & $H^{13}CO_3^-$) through the PDH enzyme complex, yielding a marker of oxidation from carbohydrate sources. In addition, following injection of pyruvate labelled with ^{13}C at the second carbon position ([2-^{13}C]pyruvate), it is possible to measure flux through the Krebs cycle, along with incorporation of acetyl-CoA into acetylcarnitine, providing a marker of L-carnitine availability. Hyperpolarized MRS therefore provides an ideal approach to explore the impact of Meldonium treatment on the diabetic heart *in vivo*.

Material And Methods

Animals

Animal studies were conducted in accordance with the UK Animals (Scientific Procedures) Act (1986) and local ethical guidelines (Medical Research Council Responsibility in the Use of Animals for Medical Research, July 1993). Thirty-six healthy male Wistar rats (~200 g) were randomly divided into four groups. All animals were fasted overnight and then either made diabetic with one intraperitoneal (i.p.) injection of streptozotocin (STZ, 55 mg/kg) or kept as controls via an injection of citrate buffer. Two weeks after STZ/citrate buffer injection, all animals were initiated on daily morning i.p. treatment with either saline or Meldonium (100 mg/kg/day). After two weeks of treatment, all animals were anesthetized with isoflurane and subjected to MRI and hyperpolarized MRS.

After three weeks of treatment, all animals were euthanized in the fed state with 5 % isoflurane vol:vol in 2 litres/min O_2, followed by removal of the heart for Langendorff perfusion, with blood and tissue collected for analysis. Blood samples, taken from the chest cavity, were centrifuged (1,200 g, 10 min, 4˚C) and plasma stored at -80˚C for later biochemical analysis. The right tibia length was measured and the kidneys and epididymal fat pads (from the posterior subcutaneous depots) were weighed[16]. The hypertrophy index (HI) was calculated as the sum of the left and right kidney weights normalized to body weight. Other investigators have previously reported HI in the literature when investigating STZ animals[17–19] as it is used as a progressive marker of diabetic renal disease. Following perfusion, the hearts were immediately freeze-clamped in liquid nitrogen and stored at -80˚C for later biochemical analysis.

CINE Magnetic Resonance Imaging (MRI)

All rodents were imaged on a 7T horizontal bore MRI instrument (Varian Medical Systems), using a 72 mm ^{1}H/^{13}C volume transmit coil and a ^{1}H four-channel phased array surface receive coil (RAPID Biomedical GmbH, Germany). Eight to ten short-axis slices (slice thickness, 1.6 mm; matrix size, 128×128; TE/TR, 4.6/1.45 ms; flip angle, 18°; number

of averages, 4) were acquired with a CINE-FLASH sequence[20]. Left ventricular volumes at end systole and end diastole were derived using the free-hand drawing function in ImageJ (NIH, USA). For each heart, left ventricular mass, ejection fraction, stroke volume and cardiac output were calculated. The average myocardial mass of the left ventricle was obtained from the average of end diastolic and end systolic masses. Stroke volume was obtained from the difference between the end diastolic and end systolic volumes. All structural and functional parameters were also indexed to body weight to account for significant differences in body weight between the control and diabetic animals.

Hyperpolarized Magnetic Resonance Spectroscopy (MRS)

Experiments were performed between 7am and 1pm when rodents were in the fed state. Samples were prepared from 40 mg of either [1-^{13}C]pyruvic acid or [2-^{13}C]pyruvic acid (Sigma), doped with 15 mM trityl radical (OXO63, GE Healthcare) and 3 µl Dotarem (1:50 dilution, Guerbet), and hyperpolarized in a prototype polarizer, with 30-40 min of microwave irradiation[14]. The sample was subsequently dissolved in a pressurized and heated alkaline solution, containing 2.4 g/l sodium hydroxide and 100 mg/l EDTA dipotassium salt (Sigma-Aldrich), to yield a solution of 80 mM hyperpolarized sodium [1-^{13}C]pyruvate or [2-^{13}C]pyruvate with a polarization of 30% or 20% respectively, at physiological temperature and pH. From the resulting solution, 1 ml was injected over 10 s via a tail vein catheter into a rat located in the 7T MRI system described above. Using the 72 mm ^{1}H/^{13}C volume transmit coil and a two-channel ^{13}C surface receive coil (RAPID Biomedical GmbH, Germany), cardiac ^{13}C spectra were acquired using a simple ECG-gated pulse-acquire spectroscopy sequence over 60 s following the injection of the hyperpolarized pyruvate (repetition time 1s; excitation flip angle 15°; sweep width 13,021 Hz; acquired points 2,048; frequency centered on the C_1 pyruvate resonance)[21].

Each rat received two injections, one with [1-^{13}C]pyruvate and one with [2-^{13}C]pyruvate, given in a random order and separated by at least one hour. Following data acquisition, the ^{13}C label from pyruvate and its metabolic products were summed over 30 s from the first appearance of pyruvate in the acquired spectra and fitted with the AMARES algorithm within jMRUI[22]. Each of the metabolites was quantified as the ratio of the metabolites to either [1-^{13}C]pyruvate or [2-^{13}C]pyruvate. In order to assess any changes within the Krebs cycle independent of changes in ^{13}C flux through PDH, all metabolites obtained from [2-^{13}C]pyruvate were normalized to pyruvate dehydrogenase flux, as calculated from the ratio of CO_2 + bicarbonate to [1-^{13}C]pyruvate measured in the [1-^{13}C]pyruvate experiment conducted in the same animal.

Langendorff Perfusions

All animals were continued on the treatment protocol for one additional week, after which hearts were excised for a Langendorff ischemia-reperfusion protocol. The hearts were cannulated and perfused with warm oxygenated Krebs-Henseleit buffer (37 ˚C) containing 11 mM glucose and 0.4 mM of palmitate, at a constant pressure of 100 mmHg as described by Heather *et al*[23]. A water-filled PVC balloon, which was connected via a polythene tube to a calibrated pressure transducer and a PowerLab data acquisition system (AD Instruments, Oxfordshire, UK), was inserted into the left ventricle to measure cardiac function. The balloon was inflated to an end-diastolic pressure of 4-8 mmHg. Hearts were subjected to 20 minutes of normal flow (t=1:20 min), followed by 30 minutes of a low-flow ischemia (0.4 ml/min/gww, t=21:50 min) and reperfused again at normal flow for another 30 minutes (t=51:80 min). The hearts were freeze-clamped with liquid nitrogen-cooled Wallenberger tongs whilst still beating on the perfusion apparatus at t=80 min.

Blood metabolites

Glucose concentrations were measured from fasted blood samples acquired at one, two- and five-weeks post-STZ injection. Insulin and non-esterified fatty acids (NEFA) were also measured in the fasted blood samples obtained five

weeks post STZ/citrate buffer injection using an enzyme-linked immunosorbent assay (Mercodia, Sweeden) and an assay kit (Randox Laboratories, UK), respectively. Terminal fed blood samples were analysed for 3-hydroxybutyrate (3-OHB), triglycerides (TAG) and lactic acid using an ABX Pentra 400 (Horiba ABX Diagnostics, California, USA). The homeostatic model assessment for insulin resistance (HOMA IR) was calculated based on fasted glucose and fasted insulin levels using the following standard formula; HOMA IR = glucose (nmol/L) x insulin (mU/L) / 22.5[24].

Metabolomics

Terminal fed blood samples were assessed for low molecular weight metabolites with Liquid Chromatography-Mass Spectrometry (LC-MS) within the Department of Chemistry, University of Oxford. Plasma samples were filtered through molecular weight cut-off filters (10kD) to remove proteins[25]. The infranatant was recovered and evaporated to dryness under reduced pressure. Sample residue was then resuspended in acetonitrile:water (95%:5%). Authenticated standards for selected acylcarnitines (up to 1.0µg/ml) were prepared using an identical method.

LC-MS: Acyl-carnitines were separated and resolved using hydrophobic-interaction liquid chromatography-mass spectrometry (HILIC). Samples were separated as previously outlined[25,26]. Briefly, samples were eluted using a binary solvent, acetonitrile:water (50%:50%) containing ammonium acetate (10mM final concentration [Solvent A]) and acetonitrile:water (95%:5%) containing ammonium acetate (10mM final concentration [Solvent B]). Samples were resolved using a linear gradient (10min: 100% Solvent A to 100% Solvent B) and re-equilibrated with 100% Solvent A. Putative compounds were identified with reference to authenticated standards for selected acyl-carnitines using retention time, accurate mass and fragmentation pattern to identify individual compounds[25]. Concentrations were calculated with reference to specific standard curves.

Statistics

All data are presented as mean ± standard deviation (SD) of the indicated number of rodents (n). Two-way ANOVA was used for assessment of the effect of STZ injection and the effect of Meldonium treatment. When an interaction term was significant in the two-way ANOVA, post-hoc multiple comparison testing using Sidak's correction was used to investigate the effect of Meldonium treatment on both the control and diabetic groups respectively. Differences between groups were considered statistically significant if $p < 0.05$.

Results

Animal Characterization

Streptozotocin (STZ) induction in male Wistar rats led to hyperglycaemia (>13 mmol/l) observed at one-week post STZ injection that gradually increased throughout the course of the experiment (Figure 1A). At five weeks post STZ injection, diabetic animals had markedly elevated glucose levels and insulin resistance (HOMA-IR) (Figure 1B). This was associated with an elevated hypertrophy index of the kidneys (Figure 1C). Daily injections with Meldonium had no significant impact on blood glucose levels, measures of insulin resistance or the kidney hypertrophy index.

Diabetic animals failed to gain weight over the course of the study, leading to a significant difference in body weight between controls and diabetics at all time-points after the initial weight matching. Lack of weight gain in the diabetic animals was attributed primarily to a reduction in fat mass as indicated by a 4.7-fold reduction in epididymal fat pad weight. There was also a small, but significant, reduction in lean mass as measured by a decreased tibia length at the terminal time-point in the diabetic animals (Figure 1F). No differences in NEFA, triglyceride or cholesterol levels were observed in the diabetic animals, however, STZ injection resulted in a significant elevation in the levels of the ketone

body, 3-hydroxybutyrate (Figure 1G-J). Meldonium treatment had no significant effect on any of the plasma metabolites assessed.

Cardiac Function

Myocardial mass was reduced by 28% in the diabetic animals compared to the control animals (Figure 2B), but this was in proportion to the change in body weight with no significant difference observed in the heart weight to body weight ratio observed (Table 1). End-diastolic volume (EDV) in the diabetic animals was reduced by 16% leading to an 18% reduction in stroke volume and, when combined with a significantly decreased heart rate, a 29% lower cardiac output in comparison to the control animals (Figure 2C-F). When differences in body weight were accounted for, this meant that a significant increase in stroke index was observed in the diabetic animals, which balanced the decrease in heart rate and lead to no significant change in cardiac index. Taken together with the lack of change in ejection fraction (Figure 2G), these structural and functional characterizations demonstrate that the diabetic hearts had no overt changes in systolic function outside of those induced by the reduction in body weight. Meldonium had no significant effect on any of the cardiac structural or functional parameters assessed.

Cardiac Metabolism

As has been previously observed[27], pyruvate dehydrogenase flux, as assessed by bicarbonate and CO_2 production from the injected hyperpolarized [1-^{13}C]pyruvate, was significantly reduced in the diabetic heart. Meldonium treatment led to a significant increase in PDH flux, by approximately 3-fold in the diabetic animals and 1.2-fold in the control animals (Figure 3C). The diabetic animals showed similar production of lactate and alanine as the controls (Figure 3D-E), although Meldonium treatment led to a small but significant elevation in lactate production in the diabetic heart.

After normalization for the differences observed in PDH flux, and thus transfer of the ^{13}C label into the TCA cycle, no significant differences in ^{13}C label incorporation into citrate or glutamate were observed in any of the groups (Figure 3F-H). However, Meldonium treatment led to a 2.1-fold reduction in the incorporation of the ^{13}C label into acetylcarnitine in both control and diabetic animals (Figure 3H), indicating a reduced availability of L-carnitine in the Meldonium treated heart.

Plasma Metabolomics

As expected, Meldonium treatment led to a significant elevation in the plasma levels of Meldonium and a significant reduction in plasma L-carnitine availability in both control and diabetic animals. This reduction was observed in addition to a significant reduction in free L-carnitine availability due to STZ-induced diabetes (Figure 4A-B). Similar patterns to those seen in free L-carnitine availability were also observed with short-chain (C3) and long-chain (C14 / C18) acylcarnitine species (Figure 4C-F). Plasma levels of all acylcarnitine species assessed are presented in Table 2.

Post-Ischemic Recovery

As a marker of cardiac function, rate pressure product (RPP) was 31% lower in the diabetic animals pre-ischemia and this functional impairment worsened post-ischemia with RPP 55% lower in the diabetic hearts (Figure 5A-C). The observed impairment in post-ischemic function in the diabetic heart was due to reductions in both systolic pressure (55% reduction) and heart rate (13% reduction) when compared with the control animals (Figure 5D-E).

However, Meldonium treatment led to a significant elevation in post-ischemic RPP by 1.3-fold in the control animals and 1.5-fold in the diabetic animals (Figure 5C). This improvement in post-ischemic function was driven by small (but non-

significant) increases in both developed pressure and heart rate in the controls (Table 3), whilst it was driven by a significant 70% elevation in systolic pressure in the diabetic hearts (Figure 5D).

Discussion

Overview

Diabetic patients are more likely to develop ischemic heart disease and suffer increased mortality and morbidity following a myocardial infarction[28]. Whilst the pathophysiology of this increased burden of disease is complex and multi-factorial, alterations in cardiac metabolism, with a shift towards reduced glucose metabolism, are considered to play a significant role. Therefore, therapeutic interventions that target elevation of glucose metabolism may offer some benefit to the diabetic population. As an example, Meldonium has been shown to be an effective anti-ischemic drug, which switches the balance of fuel utilisation away from fatty acid oxidation and towards glucose oxidation. Liepinsh *et al.* showed in type-2 diabetic rats (Goto-Kakizaki), that Meldonium could influence glucose utilisation by reducing both fed and fasted glucose levels[29]. Meldonium has been shown to work by lowering myocardial free L-carnitine and long-chain acylcarnitine by more than 60 %. This then leads to a suppression of free fatty acid oxidation which can account for the myocardial protection during ischemia[30].

Diabetes

This study has shown that, as expected, STZ-induced type-1 diabetic rats had hyperglycaemia accompanied by an elevated hypertrophy index in the kidneys. This is a common feature of STZ induced diabetes, elevated glucose levels are already known to be apparent after 2 days[31], and even though the elevated hypertrophy index is mostly accounted for by increased fluid intake, as shown by Bauman *et al.*[32], an element of increased renal mass is considered to account for the rest.

Furthermore, the STZ-injected animals had reduced body weight accompanied by both significantly smaller fat pads and reduced tibia length. Cardiac structure (LV mass) and function (stroke volume, cardiac output) were reduced in the STZ injected animals relative to controls but these changes were proportionate to the reduction in body weight. When indexed to body weight, a slight increase in stroke index was observed to balance the significant reduction in heart rate allowing the diabetic animals to maintain a normal cardiac index. As the CINE MRI techniques used in this study only allow assessment of systolic function, these findings do not exclude the possibility that there may have been an element of diastolic dysfunction, as has previously been seen in diabetic animal models when assessed using echocardiography[13]. *In vivo* metabolism, assessed with hyperpolarized magnetic resonance, showed reduced PDH flux in the STZ injected animals, which has been shown previously five days after STZ induction[27].

MeldoniumTreatment in Diabetic Animals

Meldonium treatment had minimal effects on the *in vivo* parameters assessed in the STZ-injected animals (e.g. blood glucose, body weight, insulin sensitivity, hypertrophy index etc.). Previous studies showed that Meldonium can reduce blood glucose levels in both rodent models of diabetes (STZ injection) and insulin resistant models of diabetes (Zucker obese rats), as well as in humans with type-2 diabetes[33–35]. However, treatment in those studies was continued for longer periods (4-12 weeks) than in our current study (3 weeks) and so it is possible that a longer period of treatment may have revealed these beneficial effects.

However, we did observe that Meldonium induced an increase in flux through PDH, as indicated by enhanced production of ^{13}C bicarbonate and $^{13}CO_2$ following the injection of hyperpolarized [1-^{13}C]pyruvate. In addition, the use of hyperpolarized [2-^{13}C]pyruvate revealed a reduction in L-carnitine availability through a reduced incorporation of the ^{13}C

label into acetylcarnitine. Taken together, this would suggest an increase in glucose oxidation in the Meldonium treated diabetic heart and a shift away from fatty acid oxidation. Unfortunately, we were unable to directly assess fatty acid oxidation *in vivo* as hyperpolarized MRI is currently unable to probe the oxidation of long-chain fatty acids, although development work has shown the ability of the technique to probe the oxidation of short-chain fatty acids and ketone bodies[36–38].

Improvements in post-ischemic function were observed in the *ex vivo* perfused heart with a 50% increase in RPP following a 30-minute period of low-flow ischemia. This result agrees with the work of Vilskersts *et al.*[39] and Sesti *et al.*[40] who have shown that Meldonium treatment leads to a smaller infarct size post ischemia-reperfusion. Mildronate treatment has also previously been shown to improve diastolic heart function and increase left ventricular ejection fraction in patients with type 2 diabetes, with blood glucose levels also reduced in these patients[41].The mechanistic link between these improvements and Meldonium's effect on L-carnitine availability has been demonstrated by simultaneous treatment with Meldonium and L-carnitine, which prevents these beneficial effects[42].

MeldoniumTreatment in Control Animals

Meldonium treatment induced very few effects in the healthy control animals but it increased PDH flux by 20%, likely indicating increased glucose oxidation. The mechanism for this increase would again appear to be mediated by a reduction in fatty acid oxidation due to the reduced availability of L-carnitine for transport of fatty acids into the mitochondria. In support of this, hyperpolarized MRS also revealed a reduction in mitochondrial L-carnitine availability in the control animals, as demonstrated by a reduction in the incorporation of [2-^{13}C]pyruvate into acetylcarnitine, a finding supported by significant reductions in several acylcarnitine species in the plasma, including free L-carnitine. Meldonium showed no differences in *ex vivo* cardiac function in the control hearts prior to ischemia, however after ischemia, rate pressure product (RRP) was elevated suggesting an improved recovery. Such a finding indicates that even in the control heart, a switch towards increased flux through pyruvate dehydrogenase is beneficial during reperfusion. A similar finding has previously been shown by Liu *et al.* when using the pyruvate dehydrogenase activator, dichloroacetate[43].

Conclusion

Therapeutic interventions aimed at restoring the normal balance of glucose and fatty acid oxidation in the diabetic heart have been suggested to have potential in preventing the increased cardiovascular mortality and morbidity associated with the disease. In this study, we have used the novel imaging approach of hyperpolarized magnetic resonance to show that the anti-ischemic agent, Meldonium, leads to an increase in *in vivo* flux through pyruvate dehydrogenase in both the healthy and diabetic rodent heart. This switch in fuel utilization towards more oxygen-efficient glucose metabolism may account for the improved recovery post-ischemia. Given the recent demonstration of the ability of hyperpolarized magnetic resonance to study alterations in metabolism in the human heart[44,45], there is clear potential for such studies to be translated into clinical trials assessing the potential for metabolic therapies in the diabetic heart.

Abbreviations

FA = fatty acid

gww = gram wet weight

HI = hypertrophy index

HOMA IR = homeostatic model assessment for insulin resistance

i.p. = intraperitoneal

LC-MS = liquid chromatography-mass spectrometry

Mel = meldonium

MRI = magnetic resonance imaging

MRS = magnetic resonance spectroscopy

NEFA = non esterified fatty acid

OCTN = L-carnitine transporter

PDH = pyruvate dehydrogenase

RPP = rate pressure product

STZ = streptozotocin

TAG = triglycerides

3-OHB = beta-hydroxybutyrate

Declarations

Ethics approval and consent to participate
• Consent for publication
• Availability of data and materials
• Competing interests
• Funding
• Authors' contributions
• Acknowledgements
• Authors' information (optional)

ETHICS APPROVAL AND CONSENT TO PARTICIPATE

All animal studies were conducted in accordance with the UK Animals (Scientific Procedures) Act (1986) and local ethical guidelines (Medical Research Council Responsibility in the Use of Animals for Medical Research, July 1993).

CONSENT FOR PUBLICATION

All authors consent for publication.

AVAILABILITY OF DATA AND MATERIALS

The dataset supporting the conclusions of this article is included within the article.

COMPETING INTEREST

None competing interest declared.

FUNDING

This study was funded by a grant from the Danish Council for Strategic Research entitled “LIFE-DNP: hyperpolarized magnetic resonance for in vivo quantification of lipid, sugar and amino acid metabolism in lifestyle related diseases”. DJT would also like to acknowledge financial support provided by the British Heart Foundation (BHF) in the form of a BHF Senior Research Fellowship (FS/17/58/33072). DS would like to acknowledge the financial support provided by a Novo Nordisk Postdoctoral Fellowship. DJT would also like to acknowledge the support provided by the OXFORD-BHF Centre for Research Excellence (grant RE/13/1/30181) and the NIHR Oxford Biomedical Research Centre.

AUTHORS’ CONTRIBUTIONS

DS, DJT and LCH designed the study and wrote the manuscript. DS performed the animal, molecular biology work, undertook the CINE-MRI, HP-MRS measurements. DS, VB and LH undertook the Langendorff perfusions. DS analysed the data. VB, MKC, KT and LH helped with the MR imaging. VB, MKC and KT helped with the animal work. DH performed the metabolomics, DS and DH analysed the metabolomics data. All authors read the manuscript and discussed the interpretation of the results and approved the final manuscript.

ACKNOWLEDGEMENTS

Metabolomic analysis was performed in the Department of Chemistry, University of Oxford by DH led by Associate Professor James McCullagh. DS, LCH and DJT are the guarantors of this work and, as such, had full access to all the data in the study and take responsibility for the integrity of the data and the accuracy of the data analysis.

References

1. Saeedi P, Petersohn I, Salpea P, Malanda B, Karuranga S, Unwin N, et al. Global and regional diabetes prevalence estimates for 2019 and projections for 2030 and 2045: Results from the International Diabetes Federation Diabetes Atlas, 9th edition. Diabetes Res Clin Pract [Internet]. 2019 Nov 1 [cited 2020 Apr 29];157. Available from: https://www.diabetesresearchclinicalpractice.com/article/S0168-8227(19)31230-6/fulltext
2. Federation ID. IDF Diabetes Atlas. 2017.
3. Kannel WB, McGee DL. Diabetes and Cardiovascular Disease. JAMA [Internet]. 1979 May 11 [cited 2019 Feb 11];241(19):2035. Available from: http://jama.jamanetwork.com/article.aspx?doi=10.1001/jama.1979.03290450033020
4. Jia G, Whaley-Connell A, Sowers JR. Diabetic cardiomyopathy: a hyperglycaemia- and insulin-resistance-induced heart disease. Diabetologia [Internet]. 2018 Jan [cited 2019 Feb 11];61(1):21–8. Available from: http://www.ncbi.nlm.nih.gov/pubmed/28776083
5. Soedamah-Muthu SS, Fuller JH, Mulnier HE, Raleigh VS, Lawrenson RA, Colhoun HM. All-cause mortality rates in patients with type 1 diabetes mellitus compared with a non-diabetic population from the UK general practice research database, 1992–1999. Diabetologia [Internet]. 2006 Apr 24 [cited 2019 Feb 11];49(4):660–6. Available from: http://www.ncbi.nlm.nih.gov/pubmed/16432708
6. Isfort M, Stevens SCW, Schaffer S, Jong CJ, Wold LE. Metabolic dysfunction in diabetic cardiomyopathy. Heart Fail Rev [Internet]. 2014 Jan 27 [cited 2019 Feb 11];19(1):35–48. Available from: http://www.ncbi.nlm.nih.gov/pubmed/23443849
7. Scheuermann-Freestone M, Madsen PL, Manners D, Blamire AM, Buckingham RE, Styles P, et al. Abnormal Cardiac and Skeletal Muscle Energy Metabolism in Patients With Type 2 Diabetes. Circulation [Internet]. 2003 Jun 24 [cited

2019 Feb 11];107(24):3040–6. Available from: http://www.ncbi.nlm.nih.gov/pubmed/12810608

8. Doenst T, Nguyen TD, Abel ED. Cardiac metabolism in heart failure: implications beyond ATP production. Circ Res [Internet]. 2013 Aug 30 [cited 2016 Feb 18];113(6):709–24. Available from: http://circres.ahajournals.org/content/113/6/709.full
9. Ballard F Nagele S, Bing RJ DW. Myocardial metabolism of fatty acids. J Clin Invest. 1960;39:717–23.
10. Randle PJ, Garland PB, Hales CN, Newsholme EA. THE GLUCOSE FATTY-ACID CYCLE ITS ROLE IN INSULIN SENSITIVITY AND THE METABOLIC DISTURBANCES OF DIABETES MELLITUS. Lancet. 1963;
11. Hue L, Taegtmeyer H. The Randle cycle revisited: a new head for an old hat. AJP Endocrinol Metab [Internet]. 2009;297(3):E578–91. Available from: http://ajpendo.physiology.org/cgi/doi/10.1152/ajpendo.00093.2009
12. Park S, Jeon JH, Min BK, Ha CM, Thoudam T, Park BY, et al. Role of the Pyruvate Dehydrogenase Complex in Metabolic Remodeling: Differential Pyruvate Dehydrogenase Complex Functions in Metabolism. Diabetes Metab J [Internet]. 2018 Aug [cited 2020 Jul 16];42(4):270–81. Available from: http://www.ncbi.nlm.nih.gov/pubmed/30136450
13. Le Page LM, Rider OJ, Lewis AJ, Ball V, Clarke K, Johansson E, et al. Increasing Pyruvate Dehydrogenase Flux as a Treatment for Diabetic Cardiomyopathy: A Combined 13C Hyperpolarized Magnetic Resonance and Echocardiography Study. Diabetes [Internet]. 2015 Aug [cited 2016 Aug 17];64(8):2735–43. Available from: http://www.ncbi.nlm.nih.gov/pubmed/25795215
14. Ardenkjaer-Larsen JH, Fridlund B, Gram A, Hansson G, Hansson L, Lerche MH, et al. Increase in signal-to-noise ratio of > 10,000 times in liquid-state NMR. Proc Natl Acad Sci [Internet]. 2003 Sep 2 [cited 2017 May 19];100(18):10158–63. Available from: http://www.ncbi.nlm.nih.gov/pubmed/12930897
15. Timm KN, Miller JJ, Henry JA, Tyler DJ. Cardiac applications of hyperpolarised magnetic resonance. Prog Nucl Magn Reson Spectrosc [Internet]. 2018 [cited 2020 Jun 8];106–107:66–87. Available from: http://www.ncbi.nlm.nih.gov/pubmed/31047602
16. Chusyd DE, Wang D, Huffman DM, Nagy TR. Relationships between Rodent White Adipose Fat Pads and Human White Adipose Fat Depots. Front Nutr [Internet]. 2016 Apr 19 [cited 2019 Jun 21];3:10. Available from: http://journal.frontiersin.org/Article/10.3389/fnut.2016.00010/abstract
17. Habibuddin M, Daghriri HA, Humaira T, Qahtani MS Al, Hefzi AAH. Antidiabetic effect of alcoholic extract of Caralluma sinaica L. on streptozotocin-induced diabetic rabbits. J Ethnopharmacol [Internet]. 2008 May [cited 2020 May 6];117(2):215–20. Available from: https://linkinghub.elsevier.com/retrieve/pii/S0378874108000470
18. Malatiali S, Francis I, Barac-Nieto M. Phlorizin Prevents Glomerular Hyperfiltration but not Hypertrophy in Diabetic Rats. Exp Diabetes Res [Internet]. 2008 [cited 2020 May 6];2008:1–7. Available from: http://www.hindawi.com/journals/jdr/2008/305403/
19. Lee S-I, Kim J-S, Oh S-H, Park K-Y, Lee H-G, Kim S-D. Antihyperglycemic Effect of Fomitopsis pinicola Extracts in Streptozotocin-Induced Diabetic Rats. J Med Food [Internet]. 2008 Sep [cited 2020 May 6];11(3):518–24. Available from: http://www.ncbi.nlm.nih.gov/pubmed/18800901
20. Haase A, Frahm J, Matthaei D, Hanicke W, Merboldt K-D. FLASH imaging. Rapid NMR imaging using low flip-angle pulses. J Magn Reson [Internet]. 1986 Apr 1 [cited 2019 Feb 12];67(2):258–66. Available from: https://www.sciencedirect.com/science/article/pii/0022236486904336
21. Dodd MS, Ball V, Bray R, Ashrafian H, Watkins H, Clarke K, et al. In vivo mouse cardiac hyperpolarized magnetic resonance spectroscopy. J Cardiovasc Magn Reson. 2013;
22. Vanhamme L, Van Den Boogaart A, Van Huffel S. Improved Method for Accurate and Efficient Quantification of MRS Data with Use of Prior Knowledge. J Magn Reson. 1997;

23. Heather LC, Pates KM, Atherton HJ, Cole MA, Ball DR, Evans RD, et al. Differential Translocation of the Fatty Acid Transporter, FAT/CD36, and the Glucose Transporter, GLUT4, Coordinates Changes in Cardiac Substrate Metabolism During Ischemia and Reperfusion. Circ Hear Fail [Internet]. 2013 Sep [cited 2020 May 29];6(5):1058–66. Available from: https://www.ahajournals.org/doi/10.1161/CIRCHEARTFAILURE.112.000342
24. Salgado ALF de A, Carvalho L de, Oliveira AC, Santos VN dos, Vieira JG, Parise ER. Insulin resistance index (HOMA-IR) in the differentiation of patients with non-alcoholic fatty liver disease and healthy individuals. Arq Gastroenterol [Internet]. 2010 Jun [cited 2020 May 21];47(2):165–9. Available from: http://www.scielo.br/scielo.php?script=sci_arttext&pid=S0004-28032010000200009&lng=en&tlng=en
25. Walsby-Tickle J, Gannon J, Hvinden I, Bardella C, Abboud MI, Nazeer A, et al. Anion-exchange chromatography mass spectrometry provides extensive coverage of primary metabolic pathways revealing altered metabolism in IDH1 mutant cells. Commun Biol [Internet]. 2020 Dec 20 [cited 2020 May 26];3(1):247. Available from: http://www.nature.com/articles/s42003-020-0957-6
26. Sowell J, Fuqua M, Wood T. Quantification of total and free carnitine in human plasma by hydrophilic interaction liquid chromatography tandem mass spectrometry. J Chromatogr Sci. 2011;
27. Schroeder MA, Cochlin LE, Heather LC, Clarke K, Radda GK, Tyler DJ. In vivo assessment of pyruvate dehydrogenase flux in the heart using hyperpolarized carbon-13 magnetic resonance. Proc Natl Acad Sci [Internet]. 2008 Aug 19 [cited 2019 Jun 5];105(33):12051–6. Available from: http://www.ncbi.nlm.nih.gov/pubmed/18689683
28. Howangyin KY, Silvestre J-S. Diabetes mellitus and ischemic diseases: molecular mechanisms of vascular repair dysfunction. Arterioscler Thromb Vasc Biol [Internet]. 2014 Jun [cited 2020 Jun 8];34(6):1126–35. Available from: https://www.ahajournals.org/doi/10.1161/ATVBAHA.114.303090
29. Liepinsh E, Vilskersts R, Zvejniece L, Svalbe B, Skapare E, Kuka J, et al. Protective effects of mildronate in an experimental model of type 2 diabetes in Goto-Kakizaki rats. Br J Pharmacol [Internet]. 2009 Aug;157(8):1549–56. Available from: http://doi.wiley.com/10.1111/j.1476-5381.2009.00319.x
30. Simkhovich BZ, Shutenko Z V., Meirēna D V., Khagi KB, Mežapuķe RJ, Molodchina TN, et al. 3-(2,2,2-Trimethylhydrazinium)propionate(thp)-a novel γ-butyrobetaine hydroxylase inhibitor with cardioprotective properties. Biochem Pharmacol [Internet]. 1988 Jan 15 [cited 2020 May 5];37(2):195–202. Available from: http://www.ncbi.nlm.nih.gov/pubmed/3342076
31. Rossini AA, Like AA, Chick WL, Appel MC, Cahill GF. Studies of streptozotocin induced insulitis and diabetes. Proc Natl Acad Sci U S A. 1977;
32. Bauman JW. Proteinuria in long term streptozotocin diabetes in rats. Life Sci [Internet]. 1980 Dec [cited 2020 May 5];27(22):2121–4. Available from: https://linkinghub.elsevier.com/retrieve/pii/0024320580904932
33. Sokolovska J, Isajevs S, Sugoka O, Sharipova J, Lauberte L, Svirina D, et al. Correction of glycaemia and GLUT1 level by mildronate in rat streptozotocin diabetes mellitus model. Cell Biochem Funct [Internet]. 2011 Jan [cited 2018 May 11];29(1):55–63. Available from: http://www.ncbi.nlm.nih.gov/pubmed/21264891
34. Statsenko ME, Turkina S V., Belenkova S V., Poletaeva L V., Dudchenko GP. Effects of Mildronate, as a part of combined heart failure therapy, on carbohydrate and lipid metabolism and oxidative stress parameters in patients with type 2 diabetes mellitus. Российский кардиологический журнал [Internet]. 2010 Apr 1 [cited 2020 May 5];0(2):45–51. Available from: https://doaj.org/article/86676c0ecc914ef4acadacb215742054
35. Liepinsh E, Skapare E, Svalbe B, Makrecka M, Cirule H, Dambrova M. Anti-diabetic effects of mildronate alone or in combination with metformin in obese Zucker rats. Eur J Pharmacol [Internet]. 2011 May 11 [cited 2018 Jul 12];658(2–3):277–83. Available from: https://www.sciencedirect.com/science/article/pii/S0014299911002044

36. Abdurrachim D, Woo CC, Teo XQ, Chan WX, Radda GK, Lee PTH. A new hyperpolarized 13 C ketone body probe reveals an increase in acetoacetate utilization in the diabetic rat heart. Sci Rep. 2019;
37. Miller JJ, Ball DR, Lau AZ, Tyler DJ. Hyperpolarized ketone body metabolism in the rat heart. NMR Biomed. 2018;
38. Ball DR, Rowlands B, Dodd MS, Le Page L, Ball V, Carr CA, et al. Hyperpolarized butyrate: a metabolic probe of short chain fatty acid metabolism in the heart. Magn Reson Med [Internet]. 2014 May [cited 2015 Nov 4];71(5):1663–9. Available from: http://www.pubmedcentral.nih.gov/articlerender.fcgi?artid=4238803&tool=pmcentrez&rendertype=abstract
39. Vilskersts R, Liepinsh E, Kuka J, Cirule H, Veveris M, Kalvinsh I, et al. Myocardial Infarct Size-Limiting and Anti-Arrhythmic Effects of Mildronate Orotate in the Rat Heart. Cardiovasc Drugs Ther [Internet]. 2009 Aug;23(4):281–8. Available from: http://link.springer.com/10.1007/s10557-009-6179-2
40. Sesti C, Simkhovich BZ, Kalvinsh I, Kloner RA. Mildronate, a novel fatty acid oxidation inhibitor and antianginal agent, reduces myocardial infarct size without affecting hemodynamics. J Cardiovasc Pharmacol. 2006;
41. Statsenko ME, Belenkova S V, Sporova OE, Shilina NN. [The use of mildronate in combined therapy of postinfarction chronic heart failure in patients with type 2 diabetes mellitus]. Klin Med (Mosk) [Internet]. 2007 [cited 2020 Jul 10];85(7):39–42. Available from: http://www.ncbi.nlm.nih.gov/pubmed/17882808
42. Schonekess BO, Allard MF, Lopaschuk GD. Propionyl L-Carnitine Improvement of Hypertrophied Heart Function Is Accompanied by an Increase in Carbohydrate Oxidation. Circ Res [Internet]. 1995 Oct 1 [cited 2015 Dec 15];77(4):726–34. Available from: http://circres.ahajournals.org/content/77/4/726.full
43. Liu B, Clanachan AS, Schulz R, Lopaschuk GD. Cardiac efficiency is improved after ischemia by altering both the source and fate of protons. Circ Res. 1996;
44. Rider OJ, Apps A, Miller JJJJ, Lau JYC, Lewis AJM, Peterzan MA, et al. Noninvasive in vivo assessment of cardiac metabolism in the healthy and diabetic human heart using hyperpolarized 13C MRI. Circ Res. 2020;
45. Cunningham CH, Lau JYC, Chen AP, Geraghty BJ, Perks WJ, Roifman I, et al. Hyperpolarized 13C Metabolic MRI of the Human Heart: Initial Experience. Circ Res [Internet]. 2016 Nov 11 [cited 2020 Jun 8];119(11):1177–82. Available from: http://www.ncbi.nlm.nih.gov/pubmed/27635086

Tables

Table 1

	Control (CTR)		Streptozotocin (STZ)		STZ	Meldonium	Interaction
	Saline	**Meldonium**	**Saline**	**Meldonium**	**p-value**	**p-value**	**p-value**
HW / BW	0.56±0.13	0.48±0.07	0.54±0.05	0.55±0.06	0.46	0.17	0.12
Heart Rate (HR)	370±32	380±32	310±31	310±32	**<0.0001**	0.59	0.70
End Systolic Volume / BW	0.098±0.031	0.085±0.037	0.12±0.04	0.10±0.022	0.072	0.18	0.82
End Diastolic Volume / BW	0.04±0.088	0.037±0.02	0.046±0.049	0.046±0.067	**0.0012**	0.42	0.35
Stroke Volume / BW (Stroke Index)	0.31±0.083	0.28±0.022	0.34±0.064	0.36±0.06	**0.017**	0.95	0.30
Cardiac Output / BW (Cardiac Index)	0.11±0.028	0.11±0.014	0.10±0.019	0.11±0.014	0.75	0.93	0.41

Table 2

	Control (CTR)		Streptozotocin (STZ)		STZ	Meldonium	Interaction
Metabolites [mg/ml]	**Saline**	**Meldonium**	**Saline**	**Meldonium**	**p-value**	**p-value**	**p-value**
Meldonium	0.54±0.33	40±0.17	0.55±0.17	32±22	0.51	**<0.0001**	0.51
L-carnitine	1.11±0.66	0.55±0.14	0.65±0.19	0.32±0.05	**0.026**	**0.0059**	0.41
Acetylcarnitine	3.4±01.8	15±21	1.8±0.090	2.8±6.0	0.15	0.18	0.26
C3-acylcarnitine	0.20±0.057	0.052±0.030	0.12±0.025	0.034±0.034	**0.0055**	**<0.0001**	0.061
C5-acylcarnitine	0.11±0.028	0.11±0.014	0.10±0.019	0.11±0.014	0.29	0.78	0.33
C6-acylcarnitine	12±2.7	3.6±1.8	5.2±1.4	2.6±2.1	**0.0002**	**<0.0001**	**0.0027**
C14-acylcarnitine	6.9±3.7	1.4±0.74	3.5±1.4	0.75±0.55	**0.022**	**<0.0001**	0.11
C18-acylcarnitine	2.8±2.5	1.0±0.45	1.7±0.64	1.0±0.75	0.32	**0.035**	0.35
C18:1-acylcarnitine	1.4±1.02	0.82±0.43	1.7±0.37	0.67±0.30	0.43	**0.040**	0.85

Table 3

Pre-Ischemia							
	Control (CTR)		**Streptozotocin (STZ)**		**STZ**	**Mel**	**Interaction**
	Saline	**Meldonium**	**Saline**	**Meldonium**	**p-value**	**p-value**	**p-value**
RPP [mmHg x bpm]	37,000±4,000	41,000±11,000	25,000±8,000	25,000±10,000	**0.0008**	0.57	0.57
HR [bpm]	256±25	257±25	221±20	216±31	**0.003**	0.84	0.75
Developed Pressure [mmHg]	147±20	152±40	112±31	118±48	**0.027**	0.69	0.94
Systolic Pressure [mmHg]	147±19	151±37	98±60	118±49	**0.021**	0.48	0.65
Diastolic Pressure [mmHg]	-2.0±13	2.0±7.0	-0.031±5.7	-6.4±19	0.49	0.80	0.27
Ischemia							
	Control (CTR)		**Streptozotocin (STZ)**		**STZ**	**Mel**	**Interaction**
	Saline	**Meldonium**	**Saline**	**Meldonium**	**p-value**	**p-value**	**p-value**
Systolic Pressure [mmHg]	28±15	29±20	55±25	17±12	**0.0039**	0.62	0.61
Diastolic Pressure [mmHg]	17±6	14±20	43±32	36±17	**0.0046**	0.50	0.78
Post-Ischemia							
	Control (CTR)		**Streptozotocin (STZ)**		**STZ**	**Mel**	**Interaction**
	Saline	**Meldonium**	**Saline**	**Meldonium**	**p-value**	**p-value**	**p-value**
RPP [mmHg x bpm]	32,000±8,000	40,000±13,000	14,000±8,000	21,000±7,000	**<0.0001**	**0.045**	0.82
HR [bpm]	226±19	242±44	198±31	173±22	**0.0026**	0.77	0.17
Developed Pressure [mmHg]	144±29	158±41	72±39	141±61	**0.017**	**0.025**	0.13
Systolic Pressure [mmHg]	174±16	178±27	96±44	163±46	**0.0021**	**0.013**	**0.029**
Diastolic Pressure [mmHg]	25±18	14±27	36±39	-6.4±62	0.76	0.090	0.31

Figures

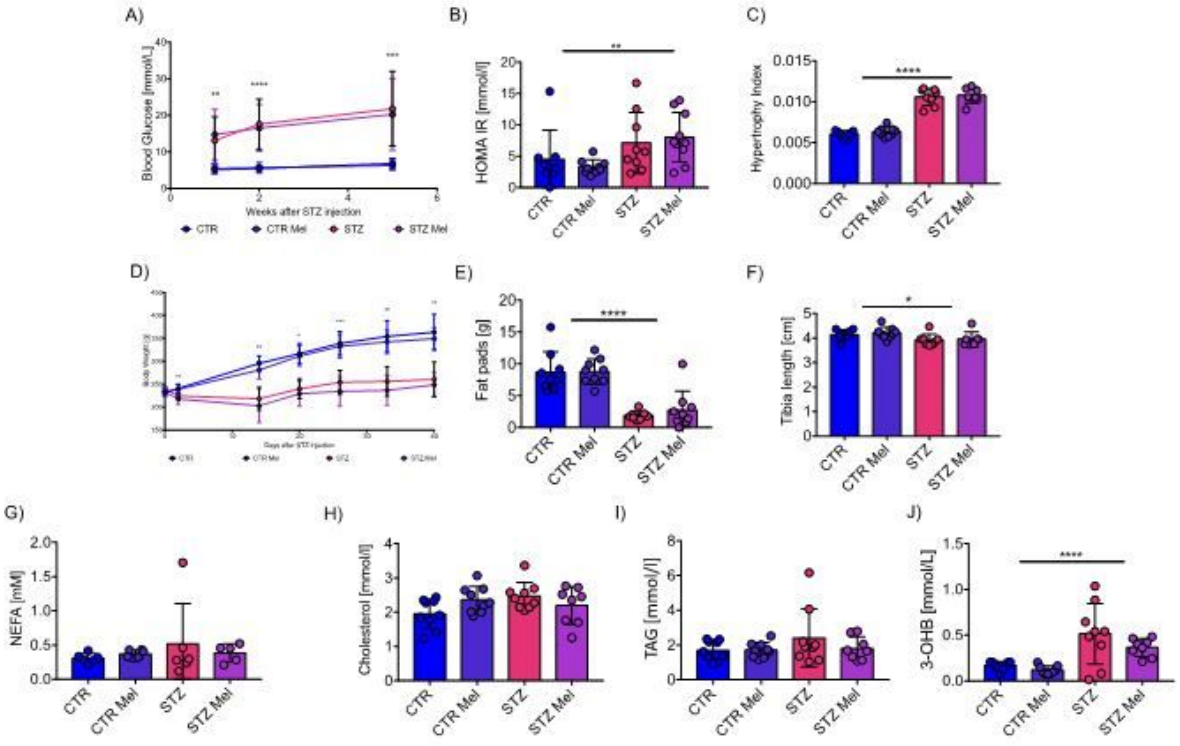

Figure 1

Animal characteristics five weeks post streptozotocin induced diabetes (STZ) compared with citrate buffer injected controls (CTR), half of all animals were treated with Meldonium (Mel) initiated at week 2 generating four different groups. (A) Fasted blood glucose concentration at 1, 2, and 5 weeks [mmol/l]. (B) Homeostatic Model Assessment for Insulin (HOMA-IR) (C) Hypertrophy index for kidneys, kidney weight normalized to body weight. (D) Weight progression over time [g] (E) Epididymal fat pad weights at 5 weeks [g]. (F) Tibia length at 5 weeks [cm]. (G) Non-esterified Fatty Acid (NEFA) levels at 5 weeks [mM]. (H) Fed cholesterol levels at 5 weeks [mmol/l]. (I) Fed triglyceride (TAG) concentrations at 5 weeks [mmol/l]. (J) Fed 3-hydroxybutyrate (3-OHB) concentrations at 5 weeks [mmol/l]. Data presented as mean ± SD. *p < 0.05, **p < 0.01, *** p < 0.001, ****p < 0.0001.

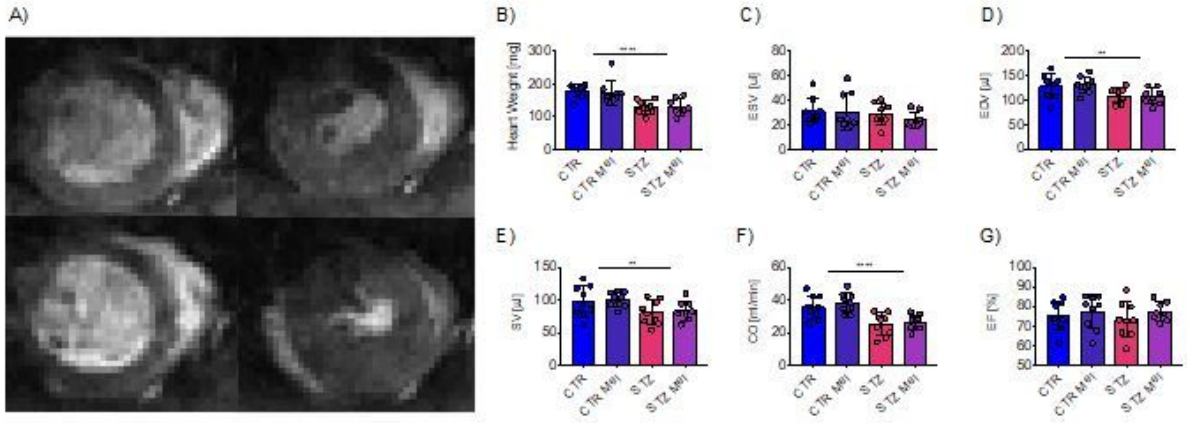

Figure 2

In vivo effects on cardiac function. (A) Example CINE MRI images from diastole to systole, short axis view. (B) Average myocardial wall mass [mg]. (C) End systolic volume (ESV) [ul]. (D) End diastolic volume (EDL) [ul]. (E) Stroke volume (SV) [ul]. (F) Cardiac Output (CO) [ml/min]. (G) Ejection Fraction (EF) [%]. Data presented as mean ± SD. *p < 0.05, **p < 0.01, ****p < 0.0001.

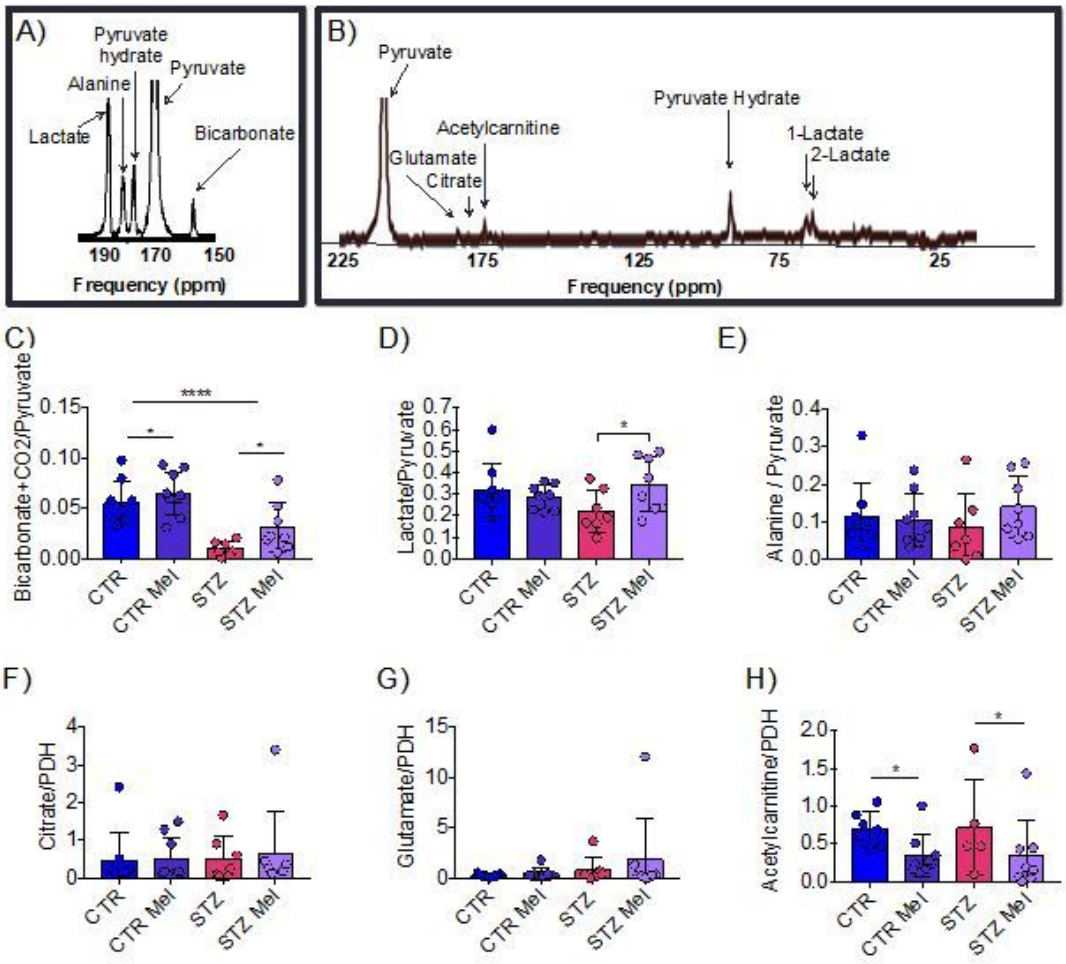

Figure 3

In vivo effects on cardiac metabolism. (A) Example of a [1-13C]pyruvate spectrum. (B) Example of a [2-13C]pyruvate spectrum. (C) Bicarbonate+CO2/pyruvate ratio, a marker of pyruvate dehydrogenase flux. (D) Lactate/pyruvate ratio. (E) Alanine/pyruvate ratio. (F) Citrate/pyruvate ratio normalized to PDH-flux. (G) Glutamate/pyruvate ratio normalized to PDH-flux. (H) Acetylcarnitine/pyruvate ratio normalized to PDH-flux. Data presented as mean ± SD. *p < 0.05, **p < 0.01, ****p < 0.0001.

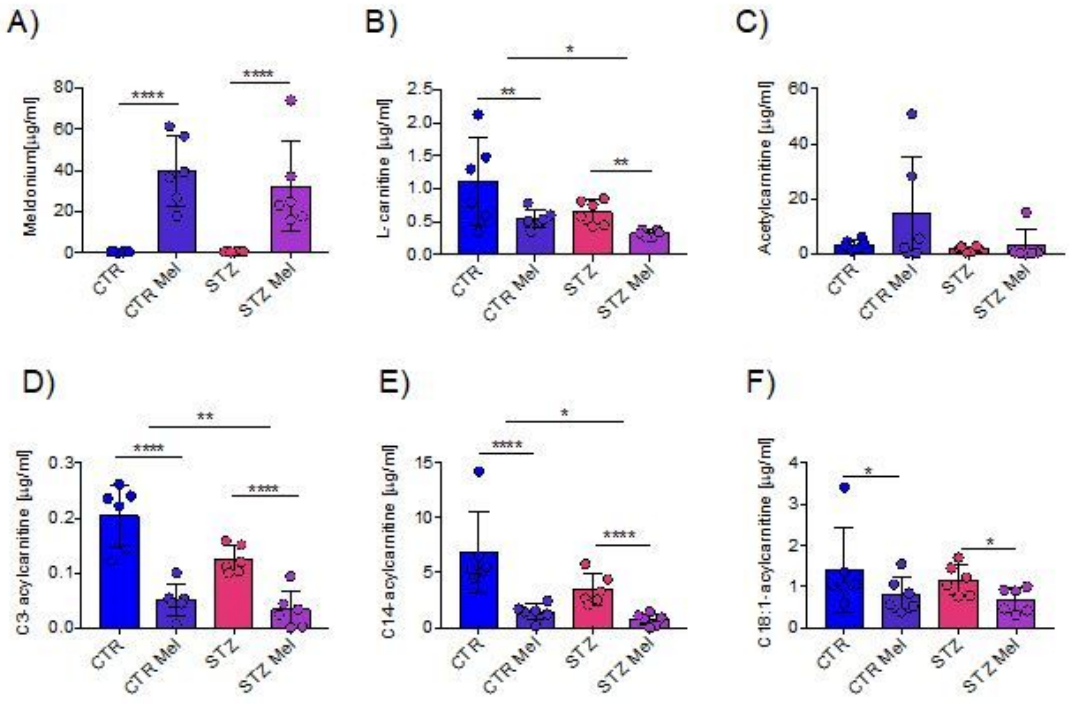

Figure 4

(A) Meldonium concentration levels in plasma [ug/ml]. (B) Free L-carnitine concentration in plasma [ug/ml]. (C) Acetylcarnitine concentration levels in plasma [ug/ml]. (D) C3-acylcarnitine (Propionylcarnitine) concentration levels in plasma [ug/ml]. (E) C14-acylcarnitine (Tetradecanoylcarnitine) concentration levels in plasma [ug/ml]. (F) C18:1-acylcarnitine (Stearoylcarnitine) concentration levels in plasma [ug/ml]. Data presented as mean ± SD. *p < 0.05, **p < 0.01, ****p < 0.0001.

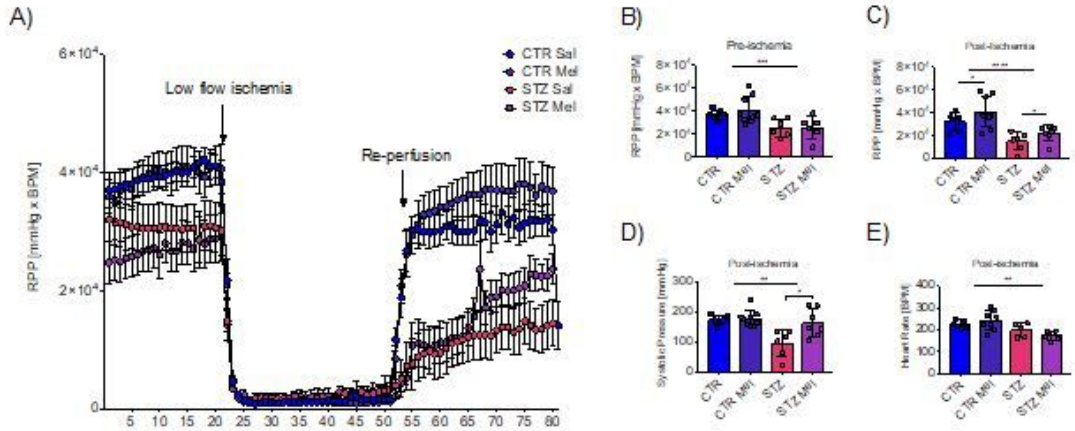

Figure 5

(A) Rate pressure product (RRP) over time [mmHg×BPM]. Pre-ischemia (t=1:20 min), low flow ischemia (t=21:50 min), post-ischemia (t=52:80 min). (B) Rate pressure product (RRP) pre-ischemia [mmHg×BPM]. (C) Rate pressure product (RRP) post-ischemia [mmHg×BPM]. (D) Developed pressure post-ischemia [mmHg]. (E) Heart rate post-ischemia [bpm]. Data presented as mean ± SD. *p < 0.05, **p < 0.01, ****p < 0.0001.